$\frac{da}{dn} = f(K, \Delta K, K_{fat.}, Y.S., \epsilon, \delta)$ process zone size

PAPER 69 (SESSION V)

A mechanical model of fatigue crack propagation

Prof. W. G. FLECK* and Prof. R. B. ANDERSON†
*Cleveland State University, Cleveland, Ohio, U.S.A.
†Carnegie-Mellon University, Pittsburgh, Pennsylvania, U.S.A.

Summary

This investigation examines the macro-behavior of cyclic fatigue crack propagation through the development of a model for the crack growth process and an experimental study of the cyclic rate of crack extension in plates of several metal alloys under various conditions of loading. The model treats cyclic crack extension in terms of the mechanical behavior of a fatigue element ahead of the crack by application of expressions for strain distribution near a crack, accumulation of cyclic damage, and a failure criterion. Specifically, the model expresses the cyclic rate of crack extension as a function of stress intensity factor range, the ratio of minimum stress intensity factor to maximum stress intensity factor, yield strength, Young's modulus, tensile ductility, endurance stress, cyclic critical stress intensity factor and a fatigue element dimension related to material grain size. The model is used to examine the relative influence of these parameters on the growth process and to correlate cyclic crack growth rate data for flat and slant modes of crack extension in sheets of four metal alloys.

Introduction

Several methods have been proposed for the correlation of the cyclic growth rate of fatigue cracks with relevant mechanical and geometrical parameters. The evaluation by Paris and Erdogan [1] of various crack propagation laws applied to a wide range of experimental data indicated that the elastic stress intensity factor, as previously suggested by Anderson and Paris [2], is a strong correlating parameter for cyclic crack extension rate data. Subsequent investigations reported by Swanson, Cicci, and Hoppe [3], Wilhem [4], Schijve [5], and others have largely substantiated the validity of the stress intensity factor correlation of growth data for a variety of materials. Hence the output of a mechanical model of the process of fatigue crack propagation under predominantly elastic conditions should be a quantitative relationship between the cyclic rate of crack growth, the stress intensity factor range, the maximum stress intensity factor, and mechanical properties of the material.

The work of McClintock and Hult [6, 7, 8] has demonstrated the dependence of the rate of fatigue crack growth on the extent of crack tip plasticity and on mechanical properties such as shear modulus, shear ductility, and yield strength. The model derived in this paper follows some of the concepts of the McClintock analysis and some approaches suggested by Rice [9] in that it describes the process of crack extension in terms of the gradual reduction of the fatigue life of a small fatigue element ahead

of an advancing crack, as it undergoes cyclic tensile straining in the region of high strain gradient near the crack front.

In the present model certain laws of tensile fatigue life and cumulative damage derived from tests of unnotched tensile fatigue specimens are applied to the fatigue element. In this way the fatigue life of the element is related quantitatively to the strain distribution ahead of a crack, the rate of accumulation of cyclic damage, and a condition for failure. Consequently the cyclic rate of extension of the crack is expressed as a function of the stress intensity factor range, the maximum stress intensity factor and material tensile properties.

The model

Consider an element of material directly ahead of a growing fatigue crack, as depicted in Fig. 1. The element is subjected to increasing values of cyclic strain range and maximum strain as the crack advances. Fatigue damage in the element begins when the strain range equals the endurance strain range of the material. The distance from the crack tip to the center of the element at this point is defined as the radius of the damage zone, r_d. The element undergoes elastic strain cycling until the crack has advanced to a distance from the element center equal to the plastic zone radius, r_p, at which point the maximum cyclic strain in the element equals the yield strain. If the material is assumed to be non-hardening, reverse plastic deformation begins when the strain range is twice the yield strain. The distance from the crack tip to the center of the element at this point is designated r_R in Fig. 1. The element suffers accumulating fatigue damage until the crack has progressed to the edge of the element and the element fractures. It is assumed that the element fails in fatigue when the crack is a distance δ, one half the element diameter, from the center of the element. The dimension δ is similar to the material structural dimension introduced by McClintock [10].

The total number of cycles to failure, N, of the fatigue element is taken to be a function of strain range, $\Delta\epsilon$, the mean strain, ϵ_m, as has been shown to be the case for tensile fatigue specimens. In this regard, it is useful to employ the fatigue life expression,

$$N = A(\Delta\epsilon - \Delta\epsilon_e)^v \tag{1}$$

proposed by Manson [11]. In equation (1) A and v are material constants and $\Delta\epsilon_e$ is the endurance strain range. For low cycle fatigue, in which $\Delta\epsilon_e/\Delta\epsilon$ is small, Sachs, *et al.*,[12] modified a fatigue life expression proposed earlier by Coffin to include the mean strain, so that

$$N = [(\epsilon_f' - \epsilon_m)/\Delta\epsilon]^2 \tag{2}$$

in which ϵ_f' is the total fatigue ductility. If Manson's suggestion of subtracting the endurance strain range from the total strain range as given in equation (1) is incorporated into equation (2), a new expression for fatigue life is obtained:

$$N = (\epsilon_f' - \epsilon_m)^2/(\Delta\epsilon - \Delta\epsilon_e)^2 \tag{3}$$

A relationship similar to equation (3) has been discussed by Coffin [13].

Because the fatigue element in the path of the crack is subjected to continually increasing values of mean strain and strain range, the accumulation of damage under the changing loading profile must be taken into account. The Palmgren-Miner cumulative damage rule is adopted for this purpose. The rule is given by

$$\sum_{i=1}^{L} \frac{n_i}{N_i} = 1 \tag{4}$$

in which L is the total number of different load levels, n_i is the number of cycles at the i^{th} load level, and N_i is the total lifetime at the i^{th} load level. If the crack advances with each cycle of loading [14], the element is subjected to a given strain level once, so that n_i equals one and L equals the total number of cycles applied to the element as the crack grows through the distance $r_d - \delta$. The average rate of growth of the crack as it traverses the damage zone can then be defined as

$$\overline{da}/dn = (r_d - \delta)/L \tag{5}$$

The damage rule applied to the fatigue element is found by combining equations (3) and (4), and is

$$\sum_{i=1}^{L} \left[\frac{\Delta\epsilon(r_i) - \Delta\epsilon_e}{\epsilon_f' - \epsilon_m(r_i)}\right]^2 = 1 \tag{6}$$

In equation (6) the strain range and mean strain are functions of the coordinate distance of the element from the crack tip. The strain range is completely elastic for $r > r_R$ as indicated in Fig. 1. If r_R is a small fraction of r_d, the elastic solution for the strain range is appropriate within most of the damage zone, and will be assumed to be valid everywhere within the damage zone. It follows that then the elastic strain range should vary inversely with the square root of the distance from the crack tip; and from the definition of the zone of reverse plastic strain, r_R, is given by

$$\Delta\epsilon_Y/\epsilon_Y = 2\sqrt{(r_R/r)} \tag{7}$$

At the edge of the damage zone the strain range equals the endurance strain range and equation (7) yields

$$\Delta\epsilon_e/\epsilon_Y = 2\sqrt{(r_R/r_d)} \tag{8}$$

Because the maximum strain is plastic for $r < r_p$ and because r_p may be a large fraction of the damage zone, it is desirable to modify the elastic solution for maximum strain to account for crack tip plasticity. There is some evidence [15, 16] from photogrid measurements of the plastic strain field near through cracks in thin sheet specimens of several aluminum alloys that, as long as the plastic zone is small relative to the crack length, the total strain can be represented approximately by

$$\epsilon_{max}/\epsilon_Y = 1 + \gamma(\sqrt{(r_p/r)} - 1) \tag{9}$$

in which γ is an empirical coefficient.

If equations (7), (8), and (9) are assumed to be applicable throughout the damage zone, they can be combined with equation (6) to yield the following expression governing the failure of a fatigue element

$$\sum_{i=1}^{L} \frac{4}{(\gamma\sqrt{(r_p/r_R)} - 1)^2}\left(\frac{\sqrt{(r_d/r_i)} - 1}{A - \sqrt{(r_d/r_i)}}\right)^2 = 1 \tag{10}$$

in which

$$A = \frac{(\epsilon_f'^p/\epsilon_Y + \gamma)\sqrt{(r_d/r_R)}}{(\gamma\sqrt{(r_p/r_R)} - 1)} \tag{11}$$

In equation (11), $\epsilon_f'^p$ is the plastic part of the total ductility. Multiplying both sides of equation (10) by $\overline{da}/dn$ and noting that as the crack advances an amount $\overline{da}/dn$ in one cycle, the distance of the element from the crack tip is reduced by an equal amount Δr, lead to a growth rate expression given by

$$\overline{da}/dn = \sum_{i=1}^{(r_d-\delta)/\Delta r} \frac{4}{(\gamma\sqrt{(r_p/r_R)} - 1)^2}\left(\frac{\sqrt{(r_d/r_i)} - 1}{A - \sqrt{(r_d/r_i)}}\right)^2 (\Delta r) \tag{12}$$

If the growth rate is small in comparison to the radius of the damage zone, the summation in equation (12) can be approximated by the integral

$$\overline{da}/dn = \int_{\delta}^{r_d} \frac{4}{(\gamma\sqrt{(r_p/r_R)} - 1)^2}\left(\frac{\sqrt{(r_d/r)} - 1}{A - \sqrt{(r_d/r)}}\right)^2 dr \tag{13}$$

Integration of equation (13) yields

$$\frac{\overline{da}/\delta}{dn} = \frac{4(r_R/r_d)\,(r_d/\delta)}{(\epsilon_f'^p/\epsilon_Y + \gamma)^2}\left[1 - \delta/r_d - \frac{2}{A}(A-1)\,(1 - \sqrt{(\delta/r_d)}\left(2 - \frac{1}{A\sqrt{(\delta/r_d)} - 1}\right) + \frac{2}{A^2}(A-3)\,(A-1)\ln\left(\frac{A-1}{A\sqrt{(\delta/r_d)} - 1}\right)\right] \tag{14}$$

The growth rate can now be related to loading and geometrical parameters by expressing r_p, r_R, and r_d in terms of corresponding stress intensity factors. The radius of the plastic zone is taken to be that derived in [9] and also in [15] after the method of Dugdale [17],

$$r_p = \pi/8(K_{max}/\sigma_Y)^2 \tag{15}$$

Under reversal of load the fatigue element deforms elastically through a stress range equal to twice the yield strength. Hence the radius of the zone of reversed plastic strain [9] is estimated by replacing K_{max} by ΔK and σ_Y by $2\sigma_Y$ in equation (15). Then

$$r_R = \pi/32(\Delta K/\sigma_Y)^2 \tag{16}$$

From equation (8) the radius of the damage zone is given by

$$r_d = 4r_R(\epsilon_Y/\Delta\epsilon_e)^2 \tag{17}$$

The endurance strain range is related to the endurance strength at zero mean stress, σ_{e_0}, and the ratio of minimum to maximum cyclic load, R, by use of the Goodman equation [18].

$$\Delta\epsilon_e/\epsilon_Y = \frac{2\sigma_{e_0}/\sigma_Y}{1 + [\sigma_{e_0}/\sigma_u]\,[(1+R)/(1-R)]} \tag{18}$$

in which σ_u is the tensile strength of the material.

It should be noted that the cyclic growth rate of equation (14) is zero when the damage zone, r_d, is as small as the fatigue element radius δ. This condition occurs when the stress intensity factor range is less than an endurance value, ΔK_e, equal to $2\sqrt{(2\delta/\pi)}\Delta\epsilon_e\,(\sigma_Y/\epsilon_Y)$, as derived from equations (16) and (17).

It can also be seen from examination of equation (14) that the growth rate becomes infinitely large when the damage zone equals $A^2\delta$. Consequently it is inferred that the coefficient γ in equations (11) and (14)

should be related to the cyclic critical stress intensity factor, K_{cc}, such that the growth rate is infinite at K_{max} equal to K_{cc}. Imposition of this criterion in equations (11) and (14) results in a value tor γ given by

$$\gamma = \frac{\epsilon_f'^p/\epsilon_Y + 1/4\sqrt{(\pi/2)}(K_{cc}/\sigma_Y\sqrt{\delta})\ (\Delta K/K_{max})}{1/2\sqrt{(\pi/2)}\ (K_{cc}/\sigma_Y\sqrt{\delta}) - 1} \qquad (19)$$

The crack extension rate is now forumulated by equations (11), and (14)-(19) in terms of K_{max}, ΔK, the material tensile properties, and the fatigue element diameter 2δ. These parameters can be arranged into six non-dimensional terms: $(da/\delta)/dn$, $\Delta K/\sigma_Y\sqrt{\delta}$, $\Delta K/K_{max}$, $\epsilon_f'^p/\epsilon_Y$, $\Delta\epsilon_e/\epsilon_Y$, and $K_{cc}/\sigma_Y\sqrt{\delta}$. The general trend of the crack extension rate as a function of stress intensity factor range, as generated by the model for some specific values of the other non-dimensional parameters, is shown in the log-log graph of Fig. 2. These curves are qualitatively similar to the trend of data reported in the literature. The lower and upper asymptotes in Fig. 2 correspond respectively to an endurance stress intensity factor range and the critical cyclic stress intensity range.

Data correlation with the model

The growth rate expression in equation (14) was used to correlate experimental data for crack extension in the slant mode for centrally-cracked sheets of 7075-T6, 6061-T6, and 2024-T3 aluminum by treating the fatigue element diameter as an empirical parameter. The other inputs to the model are the stress intensity factors and tensile material properties as listed in Table I. The results of the correlation are shown in Figs. 3-5 in which the solid lines represent equation (14). Also indicated is the point of transition to the slant mode from the flat mode of growth that was marked by the development of a shear lip in the 7075-T6 and 2024-T3 specimens. The fatigue element diameters that were used to obtain good fit to the data are $2{\cdot}2\times10^{-3}$ in for 7075-T6 and $2{\cdot}0\times10^{-3}$ in for 2024-T3, values remarkably close to average grain diameters for these materials. For 6061-T6 the fatigue element diameter was found to be about one percent of the grain diameter. In this case the dimension 2δ may be associated with subgrain formation at the crack tip, as has been observe d by Grosskreutz [19] in commercially pure aluminium.

Up to this point the model has been developed to treat crack extension in the slant mode associated with approximately plane stress conditions in the damage zone. In the flat mode of growth, however, at low stress intensities, the plastic zone is small and highly constrained. For this reason the maximum strain distribution for the flat mode is probably better approximated by the elastic solution given by

$$\epsilon_{max}/\epsilon_Y = \sqrt{(r_p/r)} \qquad (20)$$

which corresponds to setting γ equal to one in equations (9)-(14). The dashed curves in Figs. 3 and 5 show the model fit to the flat mode growth data with the same values of 2δ used in the slant mode correlation, but with the fatigue ductility treated as an empirical parameter. The lower values of ductility (refer to Table 1)for the flat mode are apparently associated with higher plastic constraint at the crack tip.

A similar correlation of flat mode growth data for 5A1-2·5Sn titanium is shown in Fig. 6. In this case the fatigue element diameter was arbitrarily set equal to the grain diameter. The flat mode ductility resulting from the data fit is substantially lower than the unconstrained tensile ductility.

The way in which the model treats the effect of sheet thickness on cyclic growth rate is seen in Fig. 7, in which data for $\frac{1}{16}$" and $\frac{1}{4}$" sheets of 7075-T6 is correlated. The slant mode model provides a reasonable fit for both thickness after transition. In the flat mode, however, different values of fatigue ductility are required for the two thicknesses. For the thicker plate, in which the plastic zone is more highly constrained, the ductility is lower.

The model is useful in correlating growth rate data over a wide range of growth rates, as shown in Fig. 8. The data in this figure is that presented by Paris in reference [20]. The material properties used in the model correlation of this data are essentially the same used to correlate the 7075-T6 data of Fig. 3, and are listed in Table 1.

Conclusions

The model of the slant mode of cyclic crack extension has been shown to correlate growth rate data for several metal alloys subjected to various combinations of load range and cyclic load over a wide spectrum of growth rates. The correlation is accomplished by use of a single empirical parameter called the fatigue element diameter that is apparently related to the size of material grains or subgrains. A flat mode model similar to the slant mode model can correlate crack growth data at low stress intensities prior to mode transition for various sheet thicknesses of the same material if the fatigue ductility is appropriately reduced. The lower fatigue ductility exhibited by growth in the flat mode is construed to be the result of increased constraint of the plastically deformed material of the crack front.

References

1. PARIS, P. and ERDOGAN, F. 'A critical analysis of crack propagation laws' Transactions of the ASME, *Joumal of Basic Engineering*, vol. 85, pp. 528-534, Dec. 1963.
2. ANDERSON, W. E. and PARIS, P. C. 'Evaluation of aircraft materials by fracture' *Metals Engineering Quarterly*, vol. 1, No. 2, p. 33, May 1961.

3. SWANSON, S. R., CICCI, F. and HOPPE, W. 'Crack propagation in clad 7079-T6 aluminum alloy sheet under constant and random amplitude fatigue loading' *Fatigue Crack Propagation*, ASTM Spec. Tech. Pub. No. 415, 1967.
4. WILHEM, D. P. 'Investigation of cyclic crack growth transitional behavior' *Fatigue Crack Propagation*, ASTM Spec. Tech. Pub. No. 415, 1967.
5. SCHIJVE, J. 'Significance of fatigue cracks in the micro-range and macro-range' *Fatigue Crack Propagation*, ASTM Spec. Tech. Pub. No. 415, 1967.
6. HULT, J. A. H. and McCLINTOCK, F. A. 'Elastic-plastic stress and strain distributions around sharp notches under repeated shear' *Proceedings of the Ninth International Congress of Applied Mechanics*, vol. 8, Brussels, pp. 51-58, 1957.
7. HULT, J. A. H. 'Fatigue crack propagation in torsion' *Journal of the Mechanics and Physics of Solids*, vol. 6, pp. 47-52, 1957.
8. McCLINTOCK, F. A. 'On the plasticity of the growth of fatigue cracks' *Fracture of Solids*, ed. Drucker and Gilman, Interscience Publishers, 1963.
9. RICE, J. R. 'The mechanics of crack tip deformation and extension by fatigue' *Fatigue Crack Propagation*, ASTM Spec. Tech. Pub. No. 415, 1967.
10. McCLINTOCK, F. A. 'Ductile fracture instability in shear' Transactions of the ASME, *Journal of Applied Mechanics*, vol. 80, pp. 582-588, Dec. 1958.
11. MANSON, S. S. 'Fatigue: a complex subject — some simple approximations' *Experimental Mechanics*, vol. 5, pp. 193-226, July 1965.
12. SACHS, G., GERBERICH, W. W., WEISS, V. and LATORRE, J. V. 'Low-cycle fatigue of pressure-vessel materials' Proceedings Am. Soc. for Testing Mats., vol. 60, pp. 512-529, 1960.
13. COFFIN, L. F., Jr. 'Cyclic strain and fatigue of metals in the creep range' Proceedings of the First International Conference on Fracture, vol. 3, p. 1543, 1966.
14. FORSYTH, P. J. E. and RYDER, D. A. 'Fatigue fracture' *Aircraft Engineering*, vol. 32, No. 374, p. 96, April 1960.
15. ANDERSON, R. B. *Plastic flow at the tip of a crack related to fracture mechanics*, Ph.D. Thesis, Carnegie-Mellon University, 1964.
16. SAWYER, S. G. *Investigation of a fracture criterion for metals*, M.S. Thesis, Carnegie-Mellon University, 1966.
17. DUGDALE, D. S. 'Yielding of steel sheets containing slits' *Journal of the Mechanics and Physics of Solids*, vol. 8, pp. 100-104, 1960.
18. DIETER, G. E. *Mechanical metallurgy*, p. 325, McGraw-Hill Book Company, Inc., 1961.
19. GROSSKREUTZ, J. C. 'Development of substructure in polycrystalline aluminum during constant-strain fatigue' *Journal of Applied Physics*, vol. 34, pp. 372-379, Feb. 1963.
20. PARIS, P. C. *The growth of cracks due to variations in load*, Ph.D. Thesis, Lehigh University, 1962.

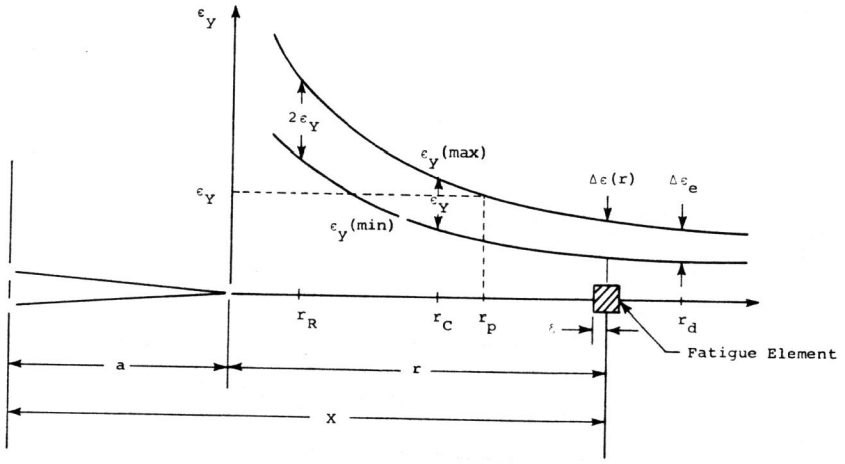

Fig. 1. Cyclic strain ahead of advancing fatigue crack.

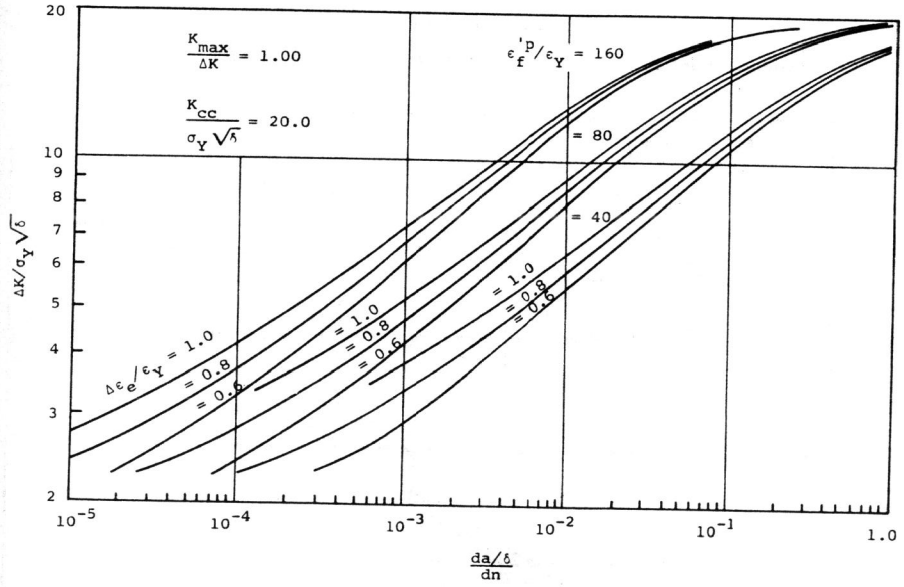

Fig. 2. Cyclic rate of crack extension as a function of stress intensity. Factor range generated by the growth model.

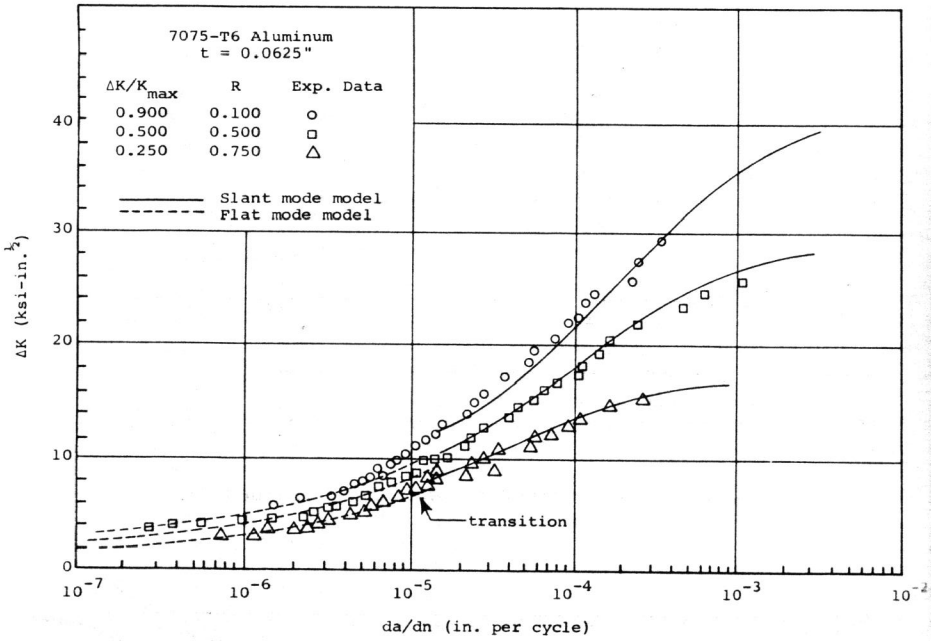

Fig. 3. Model correlation of crack growth data for 7075-T6 aluminum.

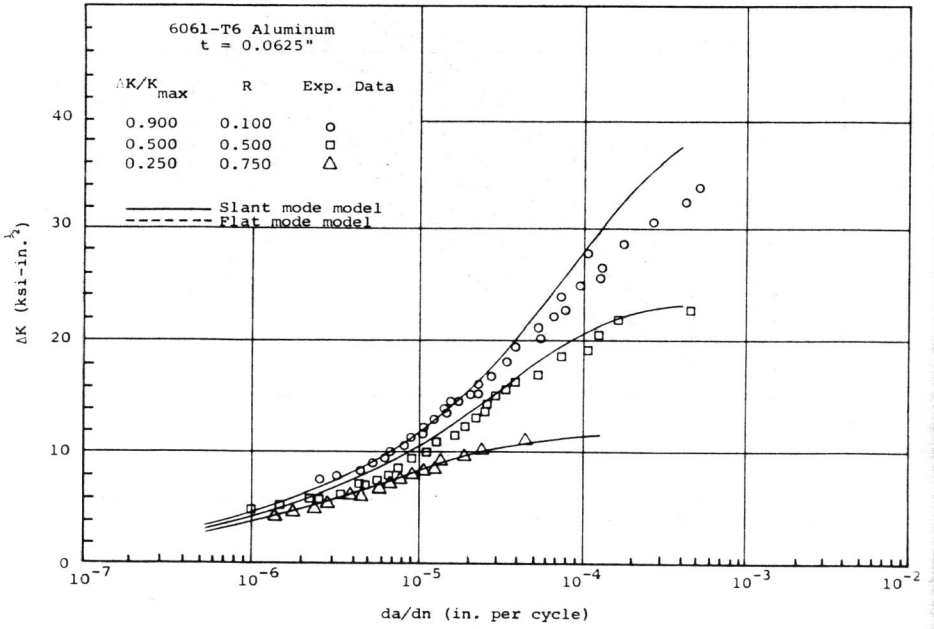

Fig. 4. Model correlation of crack growth data for 6061-T6 aluminum.

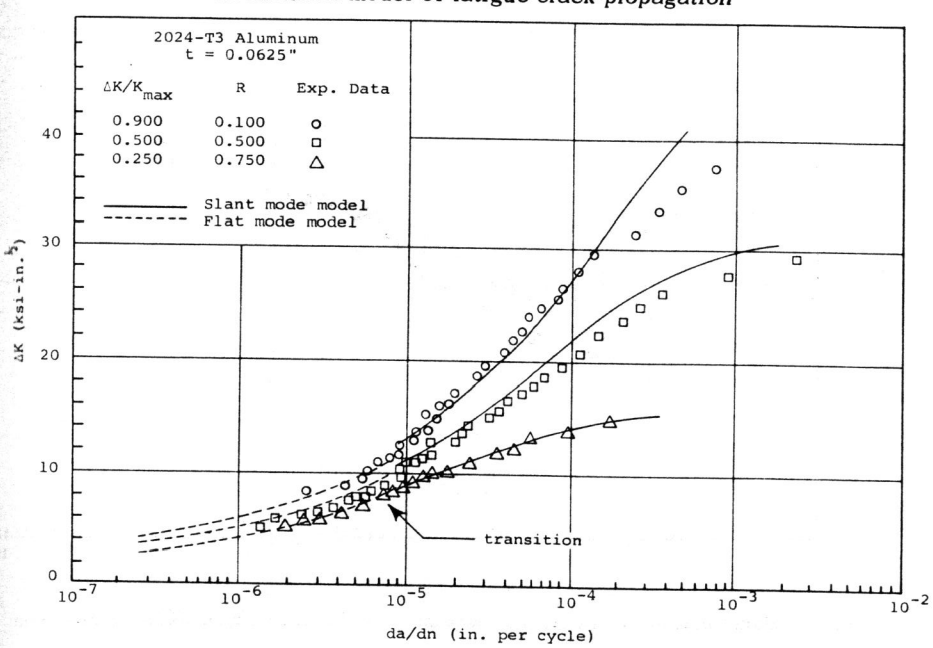

Fig. 5. Model correlation of crack growth data for 2024-T3 aluminum.

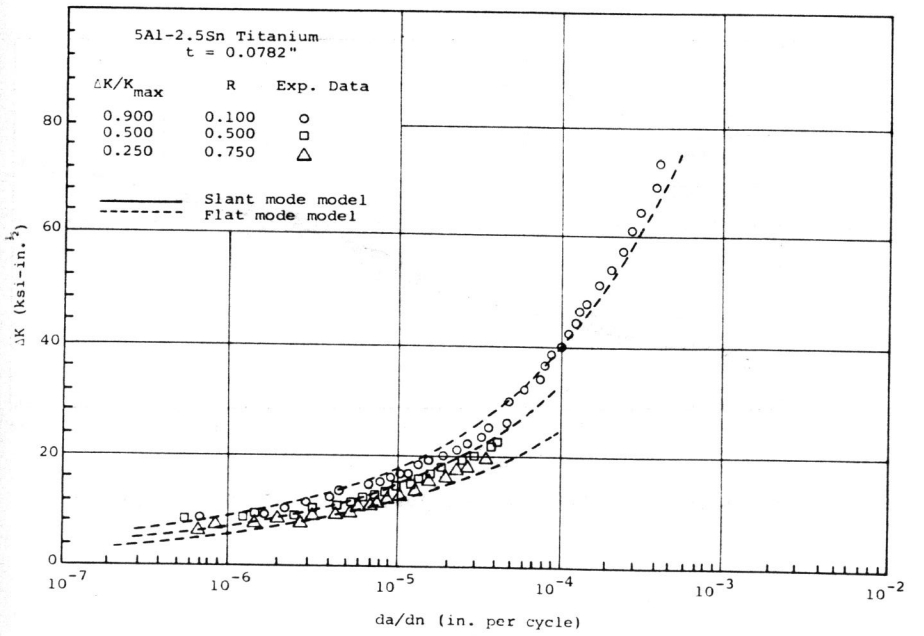

Fig. 6. Model correlation of crack growth data for 5Al-2·5 Sn titanium.

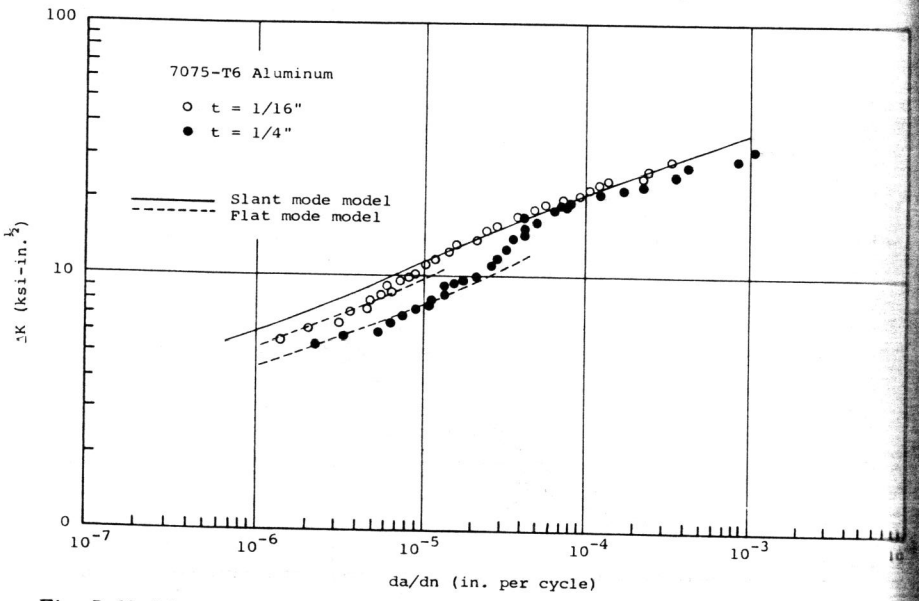

Fig. 7. Model correlation of crack growth data for 1/16 in and 1/4 in 7075-T6 aluminum.

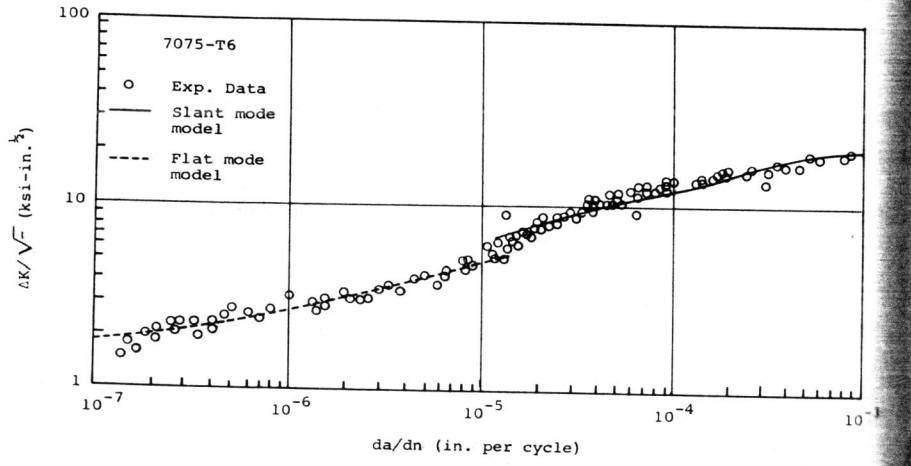

Fig. 8. Model correlation of crack growth data for 7075-T6 aluminum [20].

Table 1

Material properties used for date correlation

MATERIAL	t' (in)	σ_y (ksi)	σ_u (ksi)	σ_{eo}† (ksi)	E (psix10^{-6})	Slant Mode ϵ'_f (%)	Flat Mode ϵ'_f (%)	Apparent K_{cc} (ksi$\sqrt{in.}$)	2δ in.	Grain Size in.
7075-T6 (clad)	1/16	69.2	76.1	23.0‡	10.0	26.7*	19.5	45.2 (R=.1) 58.1 (R=.5) 70.0 (R=.75)	$2.2x10^{-3}$	$3.0x10^{-3}$
7075-T6 (ref. 20)	1/10	77.9	82.9	23.0	10.6	26.7*	15.0	45.2	$2.2x10^{-3}$	----
7075-T6	1/4	77.8	86.1	23.0	11.0	26.7	11.5	-----	$2.2x10^{-3}$	$3.0x10^{-3}$
6061-T6	1/16	43.4	47.5	13.5	11.0	58.9	----	46.3 (R=.1)** 47.5 (R=.5)** 47.5 (R=.75)**	$2.0x10^{-5}$	$2.0x10^{-3}$
2024-T3	1/16	53.0	70.5	20.0	11.2	33.4	26.0	56.9 (R=.1)** 61.8 (R=.5)** 62.9 (R=.75)**	$2.0x10^{-3}$	$2.0x10^{-3}$
5Al-2.5Sn Titanium	5/64	117.0	120.0	69.0	17.5	64.2	27.0	-----	$6.0x10^{-4}$	$6.0x10^{-4}$

† Typical handbook values
‡ Effect of cladding neglected
* Assumed same as 1/4" material
** Net section stress exceeded yield strength